Supplementary Information

High Electron Mobility of β-HgS Colloidal Quantum Dot with Doubly Occupied Quantum States

Jaekyun Kim,[a] Bitna Yoon,[b] Jaehyun Kim,[c] Yunchang Choi, [b] Young-Wan Kwon,[d] Sung Kyu Park,*[c] and Kwang Seob Jeong*[b]

[a.] *Department of Photonics and Nanoelectronics, Hanyang University, Ansan 15588, Korea*
[b.] *Department of Chemistry, Research Institute for Natural Sciences, Korea University, Seoul 02841, Korea*
[c.] *School of Electrical and Electronics Engineering, Chung-Ang University, Seoul 06974, Korea.*
[d.] *KU-KIST Graduate School of Converging Science and Technology, Korea University, Seoul 02841, Korea*

†Electronic supplementary information (ESI) available: experimental methods and additional figures, Fig. S1-3.

*Email: skpark@cau.ac.kr and kwangsjeong@korea.ac.kr.

Content

Experimental Methods

Oleylamine-HgS CQDs Synthesis

The following chemicals were purchased from Sigma-Aldrich: Bis(trimethylsilyl) sulfide ($(TMS)_2S$, synthesis grade), 1-octadecene (technical grade, 90%), oleylamine (technical grade, 70%), and tetrachloroethylene (TCE, ACS reagent, >99.0%). Ammonium chloride (NH_4Cl, 98+%), chloroform-d ($CDCl_3$, 99.8% (Isotopic), contains 0.03% v/v TMS), and mercury (II) chloride ($HgCl_2$, ACS, 99.5% min) were obtained from Alfa Aesar. Chloroform, ethanol and n-hexane (extra pure) were purchased from Daejung Chemicals. Octane (95.0%) was purchased from Samchun Chemicals. These chemicals were used without further purification. Mercury precursor was prepared by adding 160 mg of $HgCl_2$ to 8 ml of oleylamine in a three-neck flask. The mixture was degassed (~ 350 mTorr) at 85 °C for 30 min. Then, it was heated to 120 °C for 1 hour under Ar atmosphere to form the mercury-oleylamine complex. The temperature of the metal precursor has decreased to 90 °C. 0.2 ml of $(TMS)_2S$ solution (0.47 M in ODE), chalcogenide precursor, was quickly injected into the metal precursor during vigorous stirring. The reaction time was 16 min for the HgS nanocrystals described in the manuscript. The nanocrystal growth reaction was stopped by adding 50 % v/v of oleylamine in chloroform. To note, it needs very careful chemical handling especially for the mercury precursor before the chalcogenide injection.

Infrared Absorption

Mid-IR absorption spectra of HgS CQDs were obtained by using Thermoscientific Nicolet iS10 FT-IR spectrometer with resolution of 0.482 cm^{-1}. The HgS CQDs were dissolved in

tetrachloroethylene. The CQD sample was placed between CaF_2 windows with a 50 μm spacer.

X-ray Diffraction Spectroscopy

The crystal structure of HgS CQD was analyzed by using Rigaku D/Max Ultima III X-ray Diffractometer with a graphite-monochromatized Cu Kα (λ=1.54056 Å) at power settings 40 kV and 30 mA. The sample was prepared by drop-casting method. The XRD pattern was obtained from 20 ° to 60 ° with 2 °/ min scan speed.

Transmission electron microscopy: The TEM images of nanocrystals were obtained by using Tecnai G2 F30ST (FEI) microscope at 300 kV to confirm the size and shape of HgS CQDs. The sample was prepared by placing a drop of HgS CQDs on a formvar-carbon-coated Cu grid.

Proton NMR Spectroscopy

^{1}H-NMR spectra of QD-bound organic ligands were obtained using BRUKER 500 MHz spectrometer.

Electron Paramagnetic Resonance Spectroscopy (EPR Spectroscopy)

EPR spectroscopy was performed using a JEOL-JES-FA200 EPR spectrometer (X-band; 8.75-9.65 GHz; Japan) with 0.9980mW incident microwave power. The modulation width was 10 G at 100 kHz modulation frequency and the sweep magnetic field width was form 0 G to 10,000 G.

FTIR Microscopy

Infrared images were obtained by using Thermoscientific Nicolet iS50 equipped with continuum infrared microscope. The CQD film in was prepared on a gold substrate by drop-casting method. The images were taken by scanning 16 times under a resolution 8 cm^{-1} with a reflective mode.

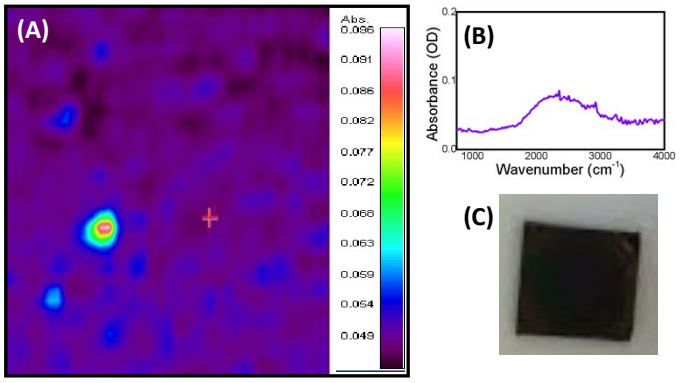

Supplementary Figure S1. (A) FTIR image of HgS CQD film (The false color indicates the absorption intensity) and (B) intraband spectrum at the marked position (red cross in the FTIR image), (C) the picture of a oleylamine-HgS CQD film.

The intraband absorption of the oleylamine-HgS CQD film and the corresponding FTIR image are shown in Fig. S1. The absorption spectrum in the inset was taken at the position marked by the red cross in the middle. The bright red spot is regarded to be randomly agglomerated nanocrystals. To facilitate the charge transport in colloidal quantum dot film, the native long organic ligands are replaced by short inorganic ligands, here thiocyanate, thereby reducing the inter-particle distance and lowering the hopping energy barrier between nanocrystals.[S1-S3] Thiocyanate is also known for maintaining the direction of the surface dipole required for heavy doping of the nanocrystals.[S4-S6]

Fabrication of CQD thin-film-transistor (TFT)

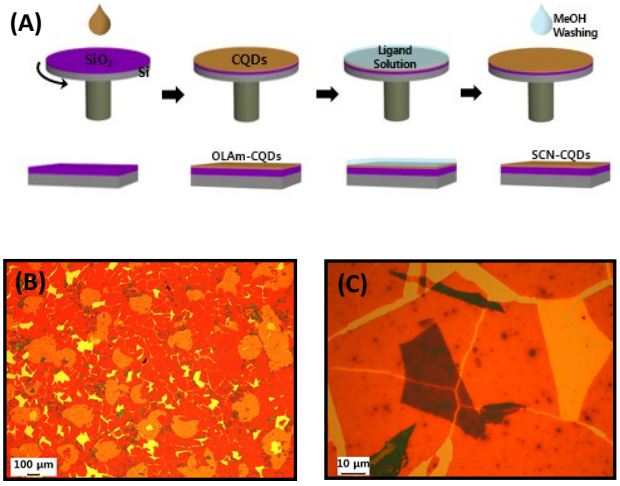

Supplementary Figure S2. (A) The schematic diagram of HgS CQD film deposition procedure for the transistor fabrication. The low (B) and high (C) magnification optical microscope (OM) images of HgS CQD films. (The morphologies of CQD films are inspected by using Nikon ECLIPSE LV100ND optical microscope.)

Fig. S2(A) illustrates the schematic diagram of the preparation procedure for the HgS CQD film transistor fabrication. First, the oleylamine passivated HgS CQDs in octane (10 mg/ml) were spin-casted on a SiO_2/Si substrate at 3,000 rpm for 30 sec. Immediately after drying, ammonium thiocyanate (NH_4SCN) solution in methanol was spin-casted on the substrate at the same rotation speed for the exchange of alkyl ligand to the short ligand and washed with methanol several times to remove residual organic unbound ligands from the CQD film. This layer-by-layer deposition procedure was repeated three times for the CQD film formation to cover the entire substrate. Finally, thermal annealing of the CQD films was carried out at the various temperature from 65 to 150 ˚C to optimize the device performance. To note, the film fabrication was processed in ambient conditions by virtue of the air-stability of the HgS CQDs. Fig S2 (B) and (C) respectively exhibit the low (left) and high (right) magnification optical microscope (OM) images of the HgS

CQD films, exhibiting their characteristic morphology with some visible voids after the ligand exchange. This often arises from shrinkage of the nanocrystal film during the ligand exchange process, consequently resulting in the efficient charge transport between CQDs with the film.[S1-S3] The ligand exchange typically leads to the reduction of the inter-particle distance and enhancement of the electrical performances. The low magnification OM image of the HgS CQD film (left) shows non-uniform regions with different contrast within the film; thicker film or multiple layers of the CQD islands are represented by darker regions. Each continuous CQD island appears to be as large as a few hundred μm^2 as seen from the high magnification OM image.

CQD thin-film-transistor (TFT) measurement

For the transistor fabrication, 50 nm-thick Al was thermally evaporated through the shadow mask for the source and drain electrode formation following the CQD film formation and subsequent thermal annealing at different temperatures. The charge carrier mobility was estimated from the linear regime of transfer curves of HgS CQD TFT devices under dark and ambient air condition by the following equation (S1):

$$\mu_{lin.} = \left(\frac{\partial I_{DS}}{\partial V_{GS}}\right)\left(\frac{L}{WC_{OX}V_{DS}}\right) \quad \text{(S1)}$$

where C_{ox}, L and W are the gate oxide capacitance per unit area, channel length and width, respectively. The semiconductor parameter analyzer (Agilent 4156C, Agilent Technologies) was employed for all the electrical measurement in this study.

Temperature Dependent Integrated intraband spectra

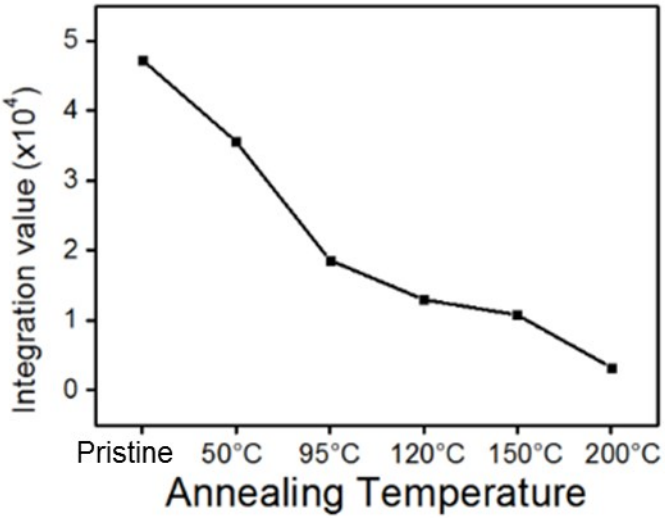

Supplementary Figure S3. Integration value of the intraband absorption peak at various temperatures.

Supporting References

[S1] A.T. Fafarman, W. K. Koh, B. T. Diroll, D. K. Kim, D. K. Ko, S. J. Oh, W. Ye, V. Doan-Nguyens, M. R. Crump, D. C. Reifsnyder, C. B. Murray and C. R. Kagan, *J. Am. Chem. Soc.*, 2011, **133**, 15753-15761.

[S2] J. M. Luther, M. Law, Q. Song, C. L. Perkins, M. C. Beard and A. J. Nozik, *ACS nano*, 2008, ***2***, 271-280.

[S3] M. V. Jarosz, V. J. Porter, B. R. Fisher, M. A. Kastner and M. G. Bawendi, *Phys. Rev. B*, 2004, **70**, 195327.

[S4] A. Robin, C. Livache, S. Ithurria, E. Lacaze, B. Dubertret and E. Lhuillier, *ACS Appl. Mater. Inter.*, 2016**, 8**, 27122-27128.

[S5] P. R. Brown, D. Kim, R. R. Lunt, N. Zhao, M. G. Bawendi, J. C. Grossman and V. Bulović, *ACS nano*, 2014, **8**, 5863-5872.

[S6] D. J. Milliron, *Nat. Mater.*, 2014, **13**, 772-773.